

## CHAPTER II

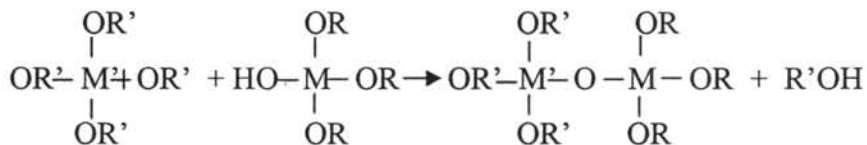
### BACKGROUND AND LITERATURE SURVEY

#### 2.1 Synthesis of Metal Alkoxide

Applications of the sol-gel processing have been increasing in recent years (Brinker, 1990). One area of particular interest is electronic ceramics. Here, the merits of the sol-gel processing, such as high purity, molecular homogeneity, and lower processing temperatures, can offer significant advantages over conventional processing method (Brinker, 1990).

The alkoxide precursors (Mazdidasni *et al.* 1986) utilized metal-organic compounds to produce high purity submicron size powders such as PLZT, BaTiO<sub>3</sub>, SrZrO<sub>3</sub>, and SrTiO<sub>3</sub>. These powders can then be used to prepare high density electronic ceramics with uniform microstructures.

Metal-organics have been also employed to prepared monolithic gels or crystalline gels of oxide materials (Mazdidasni *et al.* 1986). These gels can yield dense oxides without the need for melting or using high sintering temperatures. Some work has also been done with single component oxides such as Al<sub>2</sub>O<sub>3</sub> and TiO<sub>2</sub>(Gurkovich *et al.* 1982). Multicomponent oxide gels can be processed in a manner similar to single component oxide gels. If a multicomponent alkoxide is used, the multicomponent or complex alkoxide can be prepared by reacting a combination of single alkoxides or by adding soluble inorganic salts to single or complex alkoxides. The reaction of a partially hydrolyzed alkoxide of specie M with the alkoxide of specie M' occurs to form a double alkoxide and an alcohol as shown below (Gurkovich *et al.* 1982):



Preparing multicomponent alkoxides in this manner requires alkoxides of all species and an understanding of their relative rates of hydrolysis and reaction products. The species from an inorganic salt can be incorporated into both

multicomponent alkoxides and the alkoxide sol structure itself. If the atom or ion from the salt is to be incorporated into the sol, it must be properly dispersed and then reacted to form the multicomponent oxide. Utilizing an inorganic salt in this manner requires an understanding of the solution and the reaction chemistry of the species to obtain a stable sol of the alkoxide and of the salt. In this work, the precursors used to form lead-titanate gels, lead-zirconate gels and lead zirconate titanate gels were prepared through the reaction between a lead salt (lead glycolate precursor), titanium alkoxide (titanium glycolate precursor), and zirconium alkoxide (sodium tris (glycozirconate)). The structure of this complex alkoxide formed is important in determining the reaction chemistry of the gelling process. Some possible structures of this reaction product are shown in Fig.2.1 (Gurkovich *et al.* 1982).

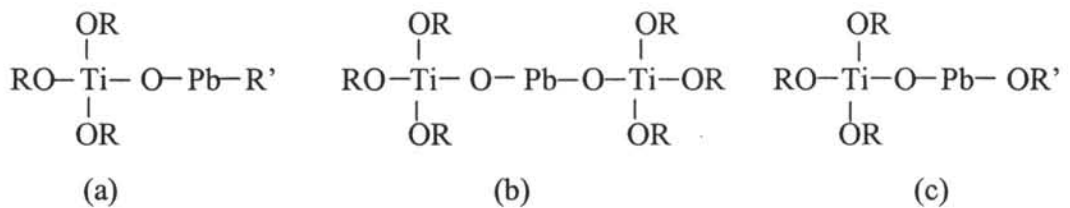


**Figure 2.1** The possible structures of gel formation.

## 2.2 Sol-Gel Process of Metal Alkoxide

The sol-gel technique has been extensively used to prepare amorphous and crystalline materials (Gurkovich *et al.* 1982). In general, the sol-gel process is the synthesis of an inorganic network at low temperatures by a chemical reaction in solution. This technique involves the phase transition characterized by a relatively rapid change from a liquid state (solution or colloidal solution) into a solid state (gel-like state).

Generally, the precursors are dissolved in a suitable organic solvent in order to form a solution. The solvent must be carefully selected so that a solution with high concentration of the required component can be obtained. Sol-gel processing involves the following steps (Budd, 1986; Yi and Sayer, 1991):

1. precursor formation
2. hydrolysis to form solution (sol)

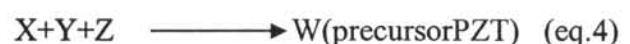
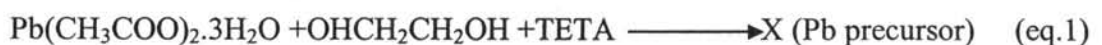
3. polycondensation
4. film and gel formation
5. organic pyrolysis by heat treatment
6. densification and crystallization by annealing process

There are two important reactions in a polymeric gel formation (Budd, 1986; Yi and Sayer, 1991). These reactions are the partial hydrolysis, followed by the condensation polymerization. Polymerization steps via hydrolysis and condensation reaction are illustrated (Budd, 1986) as follow (Yi and Sayer, 1991):



The M-O-M network product is formed by polycondensation reactions, as shown in Reactions 2.2 and 2.3 in which alcohol and water are produced as the by products. These reactions lead to a certain degree of gelation depending on the appropriate amount of water. Other critical parameters usually considered are viscosity of the solutions. Therefore, many applications of controlled hydrolysis to obtain a desired molecular structure and appropriate viscosity of the solution are employed to improve spin ability and coating ability. In addition, solution concentration, viscosity, surface tension of the solution and the deposition technique control the film thickness and uniformity (Yi and Sayer, 1991).

Sol-gel processing of  $\text{ABO}_3$ -type ceramics generally involves the following steps: (i) a preparation of a clear solution containing the A and B constituents in the required stoichiometry; (ii) a hydrolysis of the solution leading to the formation of an inorganic polymeric-(-A-B-O-)- network (gel) through condensation reactions, and (iii) a conversion of the gel by appropriate heat treatment. The sol-gel process is based on the chemistry of alkoxide:



## 2.3 Dielectric Material Properties

### Perovskite

The main perovskite structure, found in ferroelectric, antiferroelectric and piezoelectric materials, is a simple cubic structure containing three different ions of the form  $ABO_3$ . The A and B atoms represent +2 and +4 ions, respectively while the O atom is the Oxygen<sup>-2</sup> ion. This  $ABO_3$  structure in a general sense can be thought of as face centered cubic (FCC) lattice with A atoms at the corners and the O atoms on the faces. The B atom completes the picture and is located at the center of the lattice. This A atom is the largest of the atoms and consequently increases the overall size of the  $ABO_3$  (FCC) structure. As a result, there are minimum energy positions off centered from the original octahedron that can be occupied by the B atom. Shifting of this atom due to applied electric fields causes the structure to be altered, creating electric dipoles (Gustav Rose, 1830).

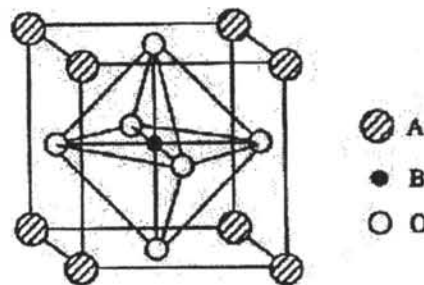


**Figure 2.2** Idealized Perovskite structure.

#### *Dodecahedral*

$Na^+, K^+, Rb^+, Ag^+, Ca^{+2}, Sr^{+2}, Ba^{+2}, Pb^{+2}, La^{+3}, Pr^{+3}, Nb^{+3}, Pi^{+3}, Ce^{+4}, Th^{+4}$

*A-site:*

#### *Octahedral*

$Li^+, Cu^{+2}, Mg^{+2}, Ti^{+3}, V^{+3}, Cr^{+3}, Mn^{+3}, Fe^{+3}, Rh^{+3}, Ti^{+4}, Mn^{+4}, Zr^{+4}, Ru^{+4}, Pt^{+4}, Nb^{+5}, Ta^{+5}, Mo^{+6}, W^{+6}, Co^{+3}, Ni^{+3}$

*B-site:*

Perovskite-type oxide group is a treasure house of various new physical properties. Superior physical properties are reported for perovskite-type and perovskite-related layered oxides, i.e. highest  $T_c$  in cuprous superconductors, highest ferroelectric  $T_c$  in perovskite-type ferroelectrics, highest ionic conductivity of proton, highest electronic conductivity in A-site deficient perovskite-type oxide (Archer *et al.*

1996). These peculiar properties originate from the three-dimensional structure which has high crystal symmetry. The stability of the structure of the perovskite-type oxides are evaluated using tolerance factor,  $t = (r_A + r_O) / \sqrt{2}(r_B + r_O)$  where  $r_i$  is the ionic radius of species  $i$ . This tolerance factor actually determines the properties of perovskite-type oxides. In case of oxides,  $r_O = 1.40 \text{ \AA}$ , so the relative ratio of  $r_A/r_B$  is the determinant factor for  $t$ . Using the ionic radii for various metal ions, we can calculate  $t$ 's for real and imaginary perovskite-type oxides. The  $t \sim 1$  has an ideal cubic perovskite type structure with the space group  $Pm\bar{3}m$  (Mitsuru, 1997). The other most common perovskite is the orthorhombic form. Different crystal structures are possible: cubic, tetragonal, orthorhombic, and rhombohedral. The distorted octahedral structures are coupled together, and a very large spontaneous polarization results from a large dielectric constant with sensitive temperature dependence. Since  $\pi$  or  $\sigma$  bonding between oxygen and metal ions are important in the electronic conductors, the energy levels of  $O_{2p}$  and  $M_{3d}$  are crucial factors for the evolution of metallic conductivity.

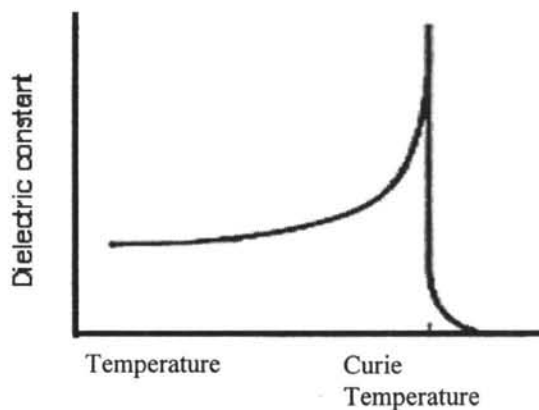


**Figure 2.3** The Curie temperature of dielectric materials.

The perovskite crystal structure which occurs in barium titanate also occurs in the alloys of the system  $PbZrO_3$ - $PbTiO_3$ , the lead zirconate titanate. By varying the ratio of Zr to Ti, the properties can be engineered to meet many transducer specifications. The phase diagram of PZT is shown in Fig.2.4 (Braithwaite, 1990).

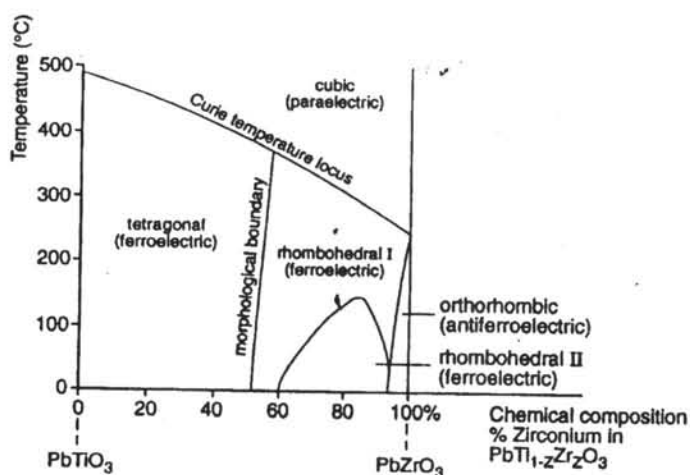


**Figure 2.4** Structural phase diagram of PZT-lead zirconate titanate.

The properties of PZT can be strongly influenced by the addition of other metal oxides. These are used to manipulate properties such as conductivity, electric coercivity and elastic modulus. In the PZT compounds, the energy conversion efficiency also depends on the chemical composition. If the composition is close to the rhombohedral-tetragonal transition, which occurs at about 50% Zr, 50%Ti, then the energy conversion efficiency rises to about 25% (the coupling coefficient ( $k$ ) = 0.5) from values in the range of 2% ( $k = 0.15$ ); and values of 50% ( $k = 0.7$ ) have been achieved in some cases (Braithwaite, 1990). The reason for this high conversion efficiency at 50% Zr-50% Ti composition is that the grains of the material can transform between the rhombohedral and tetragonal crystal classes because the energy is finely balanced between these two crystal structures at this composition. These shear transformations therefore occur, as well as the conventional electric polarization rotations, within either the rhombohedral or the tetragonal crystal grains. This allows the rotations to proceed more easily via the two mechanisms and results in smaller internal energy losses. The PZT class ferroelectrics are important because of the diversity of properties displayed by these compounds. The material properties can be engineered by chemical additions and or by a control of microstructure. This diversity of ferroelectric properties makes the materials very versatile and of crucial importance to ferroelectricity (Butterworths, 1990).

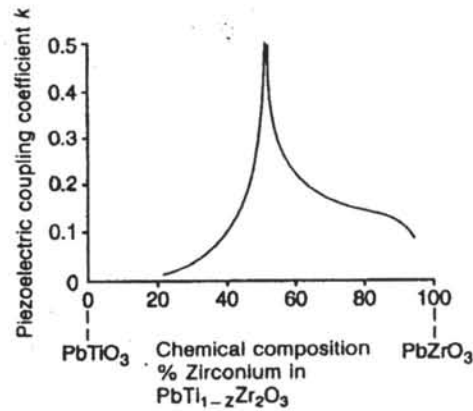


**Figure 2.5** Piezoelectric coupling coefficient and chemical composition.

**Dielectric materials can be divided into two classes** (Cardarelli, 1966):

Class I Dielectrics or Linear Dielectrics

This group identifies the linear dielectric. These materials display the most stable characteristics, as they are non-ferroelectric or paraelectric formulations, show a linear relationship of polarization to voltage, and are formulated to have a linear temperature coefficient of capacitance. These materials are primarily of rutile type ( $TiO_2$ ), and therefore exhibit lower relative dielectric permittivity ( $<150$ ) but more importantly, also lower dielectric loss and no reduction of capacitance with time. These properties, along with negligible dependence of capacitance on voltage or frequency, make these dielectrics useful in capacitor applications where close tolerance and stability are required. Linear dielectrics are also referred to as temperature compensating, as the temperature coefficient can be modified to give predictable slopes of the temperature coefficient over the standard  $-55^\circ C$  to  $+125^\circ C$  range. A flat slope, neither positive nor negative, is denoted NPO and is one of the most common of all dielectric characteristics. The extended temperature compensating ceramics are a sub-group of formulations which utilize small additions of other ferroelectric oxides such as  $CaTiO_3$  or  $SrTiO_3$  and which display near-linear and predictable temperature characteristics with relative dielectric permittivity ranging up to 500. Both categories are used in circuitry requiring stability of the capacitor (i.e., negligible aging rate, low loss, no change in capacitance with frequency or voltage, and predictable linear capacitance change with temperature).

Class II Dielectrics or Ferroelectrics

Class II dielectrics comprise the ferroelectrics. These materials offer much higher dielectric constants than Class I dielectrics, but with less stable properties with temperature, voltage, frequency, and time. The diverse range of properties of the ferroelectric ceramics requires a sub-classification into two categories, defined by temperature characteristics. (1) Stable class II: these types of materials display a maximum capacitance temperature coefficient of  $\pm 15\%$  from  $25^{\circ}\text{C}$  reference over the temperature range from  $-55^{\circ}\text{C}$  to  $+125^{\circ}\text{C}$ . These materials typically have relative dielectric permittivity ranging from 600 to 4000. (2) High relative dielectric permittivity Class II dielectrics: these capacitors have steep temperature coefficients, due to the fact that the Curie point is shifted towards room temperature for maximization of the dielectric constant. These bodies have dielectric constants from 4000 to 28,000, typically. It is important to note that ceramic capacitors made with ferroelectric formulations display a decay of capacitance and dielectric loss with time. This phenomenon, called aging, is reversible and occurs due to the crystal structure and to its change with temperature.

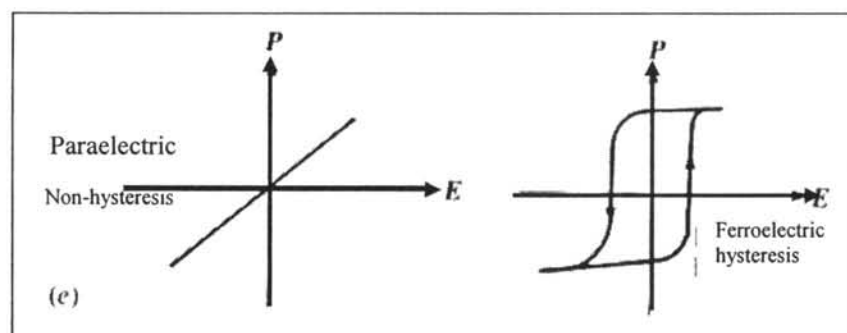


**Figure 2.6** The hysteresis loop of paraelectric and ferroelectric.

### **Ferroelectrics** (Kingery, 1991)

Ferroelectricity is defined as the spontaneous alignment of electric dipoles by their mutual interaction. This is a process parallel to spontaneous alignment of magnetic dipoles observed in ferromagnetism and derives its name from its similarity and features analogous to that process. The source of ferroelectricity arises from the fact that the local field  $E'$  increases in proportion to the polarization. For a material containing electric dipoles increased polarization increases the local field;



spontaneous polarization is to be expected at some low temperature at which the randomizing effect of thermal energy is overcome, and all the electric dipoles line up in parallel arrays.

The general source of spontaneous polarization is apparent from the defining equation for polarization, eq.2.1

$$P = (k'-1)\epsilon_0 E = N\alpha E' \quad \text{eq.2.1}$$

By introducing the Mosotti field (eq.2.2) for the local field:

$$E' = E + P/3\epsilon_0 \quad \text{eq.2.2}$$

We obtain for the polarization and the electric susceptibility:

$$P = \frac{N\alpha E}{1 - N\alpha/3\epsilon_0} \quad \text{eq.2.3}$$

When the polarizability term in the denominator,  $N\alpha/3\epsilon_0$ , approaches unity, the polarizability and susceptibility must approach infinity.

The orientation polarizability of a dipole is inversely proportional to temperature according to the relation:

$$\alpha_0 = C/kT \quad \text{eq.2.4}$$

If we consider systems in which the orientation polarizability is much larger than that for the electronic and ionic portions, a critical temperature is reached at which

$$N\alpha/3\epsilon_0 = (N/3\epsilon_0)(C/kT_c) = 1 \quad \text{eq.2.5}$$

This fixes the critical temperature as

$$T_c = NC/3\epsilon_0 = N\alpha_0 T/3\epsilon_0 \quad \text{eq.2.6}$$

Below this temperature, the Curie temperature, spontaneous polarization sets in and all the elementary dipoles have the same orientation.

Combining eqs.2.4 and 2.5 with eq.2.6 gives for the susceptibility (and dielectric constant and polarization)

$$\chi = k' - 1 = P/\epsilon_0 E = 3T_c/T - T_c \quad \text{eq.2.7}$$

This linear dependence of the inverse susceptibility on  $T - T_c$  is known as the Curie-Weiss law, and  $T_c$  is the Curie temperature.

The paraelectric phase occurs at higher temperatures, above the Curie point. The Curie point itself depends on the chemical composition of the material. In the paraelectric phase, polarization is induced by application of an electric field, but

when the field is removed it reverts to the unpolarized condition. In this phase, the electric dipole vectors are disordered in the absence of an applied field. This is analogous to the behavior of the magnetization of a paramagnet when subjected to a magnetic field.

Above the Curie temperature, since the electric dipoles are randomly oriented, no ferroelectric domains can exist. Once the material has been cooled below its Curie temperature, it becomes ferroelectric with localized spontaneous polarization within the domains.

**Antiferroelectrics** (Cardarelli, 1966):

The pure  $\text{PbZrO}_3$  exhibits an orthorhombic, and below the Curie temperature it is antiferroelectric; which means that the neighbouring unit cells of the crystal have polarizations in opposite directions. It transforms to cubic at around  $230^\circ\text{C}$ . Lead zirconate is also a candidate material for energy storage applications due to its antiferroelectric to ferroelectric transition (Fang *et al.* 1998). This is analogous to the antiferromagnetic phase in magnetic materials (David, 1995).

**Piezoelectrics** (Cardarelli, 1966):

Piezoelectric materials are those which display a two-sided relationship of mechanical stress and polarization, which is attributed to crystal lattice configurations which lack a center of symmetry. Upon compression, the centers of charge shift and produce a dipole moment, resulting in polarization. This effect is a true linear coupling, as the elastic strain observed is directly proportional to the applied field intensity, and the polarization obtained is directly proportional to the applied mechanical stress. For instance, barium titanate or lead titanate zirconate, the major constituent of ferroelectric dielectrics, lacks a center of symmetry in the crystal lattice at temperatures below the Curie point, the crystal lattice changes from tetragonal to the cubic configuration, which possesses a center of symmetry, and piezoelectric effects are no longer observed.

## 2.4 Literature Review

Perovskite structure of lead titanate (ferroelectric):

Many synthetic strategies have been employed in preparation of perovskite phase mixed metal oxides from molecular precursors for use in ferroelectric,

piezoelectric and pyroelectric devices. A popular strategy involves the reaction of individual sources of each metal required in the final material, often metal carboxylate and metal alkoxide compounds, and the subsequent calcination of the reaction products to form the corresponding perovskite phase material. Archer *et al.* (1996) studied the role of precursor segregation in the formation of perovskite phase  $\text{PbTiO}_3$  from lead oxy glycolate  $\text{Pb}(\text{OCH}_2\text{CH}_2\text{O})_2$  and phenoxyglycolate compounds. The lead precursors were synthesized by refluxing the lead carbonate with the appropriate carboxylic acid in water. The lead titanate materials were formed at low temperatures ( $300^\circ\text{--}400^\circ\text{C}$ ) by a thermolysis of the product reaction in pyridine. However, some of the experiments were complicated by the different solubilities of the reagents, making interpretation of the results ambiguous.

Fang *et al.* (1999) prepared ultrafine lead titanate powders by the co-precipitation, the microemulsion-refined freeze drying, and the microemulsion-refined co-precipitation. They found lead titanate powders in tetragonal form have been successfully prepared via three processing routes by using lead (II) nitrate and titanium (IV) chloride as starting materials. The microemulsion-refined co-precipitate is the technique which results in the formation of the finest lead titanate powder among the three processing routes investigated. However, they have to use high temperature to obtain tetragonal formation. Gelabert *et al.* (2000) studied to synthesize lead titanate from complexed precursor solutions by using lead titanate from chelated titanium and lead in alkaline aqueous solution in a hydrothermal autoclave at  $200^\circ\text{C}$  for 4-6 days. The products were identified as tetragonal perovskite-type  $\text{PbTiO}_3$  upon a heat treatment around  $200^\circ\text{C}$  for several days. This is the mild process better than that of conventional hydrothermal routes, which require higher than  $500^\circ\text{C}$  and 1000 psi to grow crystals of comparable size, but it takes a long time. So, the suitable process for preparation dielectric materials is sol-gel transition process. The sol-gel process was employed to hydrolyze and condense alkoxide precursors because of its product homogeneity and to control physical and chemical characteristics (i.e. morphology, distribution, phase transformation, electrical properties). In addition to, the sol-gel process can be employed at low temperature and shorter time to do the experiment. Li *et al.* (1993) studied the synthesis of lead titanate powders derived from a hydrothermal treatment; lead

acetate and titanium butoxide were used as starting materials mixed with PVP and PEG as additives in an autoclave apparatus at temperature 180°C to 240°C for 1-4 h. If they obtain around 100% perovskite structure, they take about 18 hr for experimental soaking time to do that. Furthermore, the suitable mol ratio between Pb and Ti should be 1:1, they obtained Pb/Ti = 2 which means PbTiO<sub>3</sub>.TiO<sub>2</sub>. Gurkovich *et al.* (1982) prepared a transparent monolithic lead titanate by a sol-gel process. The reaction of lead acetate and titanium isopropoxide in methoxyethanol was carried out at 124°C. The structure of the complex alkoxide appeared to be a long chain, high molecular weight molecule, and of high viscosity, but attempts at distillation of the solution were unsuccessful. The cracking caused by the tetragonal to cubic phase transformation of PbTiO<sub>3</sub> occurred at 490°C. Further, direct characterization will allow a better understanding of the structure. This is an important consideration in refining the technique for preparing the complex alkoxide. Tartaj *et al.* (2001) prepared a lead titanate by a sol-gel method using titanium tetrabutoxide in isopropanol and lead acetate in glacial acetic acid with stoichiometric proportion of 1:1 in volume. Both solutions were mixed at room temperature under constant stirring during 24 hours to ensure the formation of an intermediate precursor phase based on Pb-O-Ti bonding. Zeng *et al.* (2003) prepared a nanocrystalline lead titanate by an accelerated sol-gel process. The gel formation produced by lead acetate and titanium butoxide in CH<sub>3</sub>CHOHCH<sub>3</sub> was at the mol ratio of 1:1. The tetragonal perovskite structure PbTiO<sub>3</sub> was prepared at 550°C. The dimension of particles was about 50 nm.

Perovskite structure of lead zirconate (antiferroelectric):

Djuricic *et al.* (1995) studied the properties of zirconia powder produced by homogeneous precipitation by using zirconium sulphate tetrahydrate as starting material to react with polyvinylpyrrolidone in water solution and then calcined at 300°C. They received spherical particles of zirconia. The most interesting findings were the development of fully crystalline tetragonal zirconia at temperatures as low as 300°C and the existence of the metastable zirconia in domains of up to 100 nm in diameter. Jiye *et al.* (1998) studied the synthesis of and characterized ultrafine lead zirconate powders via three processes of the conventional solid reaction, the conventional co-precipitation, and the micro emulsion-refined coprecipitation from

400°C to 1000°C using either oxalic acid or an ammonia solution as the precipitant. The microemulsion-derived precursors exhibit a lower formation temperature at 600°C for orthorhombic lead zirconate than the conventionally coprecipitated precursors. Ammonia solution appears to be a more attractive precipitant than oxalic acid in reducing the formation temperature for lead zirconate. The microemulsion-derived lead zirconate powders, which are of dimension in the range of nanometers, are much finer in particle size and lower in particle agglomeration than the conventionally coprecipitated powders. Furuta *et al.* (1999) investigated the phase transitions in  $\text{PbZrO}_3$  under high pressure by Raman scattering. A polycrystalline fine-powder sample of  $\text{PbZrO}_3$  (325 mesh, 99.7% purity) was used to study phase transitions. Kobayashi *et al.* (1999) characterized  $\text{PbZrO}_3$  at high pressure by using x-ray diffraction for a phase transformation and measured dielectric constant. The lead zirconate went through the phase transformation from the orthorhombic form to the monoclinic form and possessed a dielectric constant of approximately 500 at 1.0 kHz. The Curie temperature occurred at 230°C in the cubic form. Pradhan *et al.* (2001) synthesized the stoichiometric lead zirconate at low temperature 600°C by the co-precipitation in a non-aqueous medium. The lead acetate and zirconium oxychloride were used as starting materials in NaOH- ethylene glycol solution at 60°C, 24 h, and then calcined at 600°C. They obtained lead zirconate crystalline structure at 600°C. Tang *et al.* (2003) reported lead zirconate thin films by using lead acetate trihydrate  $\text{Pb}(\text{CH}_3\text{COO})_2 \cdot 3\text{H}_2\text{O}$  mixed with zirconium n-propoxide  $\text{Zr}(\text{O}(\text{CH}_2)_2\text{CH}_3)_4$  in 2-methoxyethanol solution. Lead zirconate thin films were grown on platinum-coated silicon substrates by a chemical solution deposition. The precursor solution for spin-coating was prepared from lead acetate trihydrate and zirconium oxynitrate dihydrate as starting materials. The perovskite lead zirconate thin films have been obtained. At 100 kHz., the dielectric constant and dissipation factor of lead zirconate film are 300 and 0.020, respectively.

Perovskite structure of lead zirconate titanate (piezoelectric):

Abothu *et al.* (1999) synthesized  $\text{Pb}(\text{Zr}_{0.52}\text{Ti}_{0.48})\text{O}_3$  or PZT from microwave and conventional hydrothermal powders. PZT perovskite powders were synthesized without using excess lead content by the microwave hydrothermal method at 122°C and the conventional hydrothermal method at 138°C, sintered at 1250°C for 4 h. A

maximum permittivity of 20,570, low dissipation factor of 0.002 at 1 kHz and Curie temperature 373°C were observed for sintered pellets prepared from PZT powders obtained by microwave hydrothermal method. The pellets prepared from PZT powders sintered 1250°C for 4 h obtained by the conventional hydrothermal method showed a relative permittivity of 16,310, a dissipation factor of 0.001 at 1kHz, and the Curie temperature of 351°C. Junmin *et al.* (2000) synthesized lead zirconate titanate from an amorphous precursor by a mechanical activation. The resulting PZT powder was well dispersed, and the particle size was in the range of 30-50 nm by using SEM and TEM. The density of PZT was 97.6% at 1150°C for 1h. Sintered PZT ceramic exhibited a dielectric constant of 927 at room temperature and a peak dielectric constant of  $\cong 9100$  at the Curie point of 380°C when measured at the frequency of 1 kHz. Rabindra *et al.* (2000) prepared nanocrystalline PZT powder from the solution of Ti(IV),Zr(IV), Pb(II) ions complexed with organic acids and amines. The PZT (60/40) powders were calcined from 375°C to 600°C. The corresponding average particle sizes were 60, 30, and 25 nm along with calcination temperature at 600°C, 400°C, 200°C respectively. Kong *et al.* (2001) studied lead zirconate titanate  $\text{Pb}(\text{Zr}_{0.52}\text{Ti}_{0.48})\text{O}_3$  or PZT ceramics directly prepared from their oxide mixtures and treated by a high-energy ball milling process. X-ray diffraction result indicated that there was no reaction between the component oxides during the milling process. The particle size of the mixture was greatly reduced to nanometer scale by the milling process. PZT ceramics sintered at 1000°C for 4 h exhibited a dielectric constant of 1156 and dielectric loss of 0.03, a remnant polarization of 29  $\mu\text{C}/\text{cm}^2$  and a coercive field of 18.4 kV/cm. Wanda *et al.* (2001) studied electrical characterization of lead zirconate titanate with composition Zr/Ti  $\approx 53/47$  prepared by the organic solution route. Dielectric constants were 4000 to 8000 sintered at 1100°C for 6 h at 100 kHz. Das *et al.* (2001) prepared and characterized fine PZT powders with a molar composition 60/40 from mixed metal nitrate ( $\text{Zr}^{4+}, \text{Ti}^{4+}, \text{Pb}^{2+}$ )-polyvinyl alcohol (PVA) solution. Calcination of the precursors at 500°-600°C/2h produced single phase PZT. The dielectric constant was 10,000 at constant frequency 10 kHz. The Curie temperature showed at 385°C. Mandal *et al.* (2003) synthesized  $\text{Pb}(\text{Zr}_{0.7}\text{Ti}_{0.3})\text{O}_3$  nanoparticles in a new tetragonal crystal structure with a polymer

precursor (PVA). It formed a single phase compound of  $\text{Pb}(\text{Zr}_{0.7}\text{Ti}_{0.3})\text{O}_3$  nanoparticles calcined at  $400^\circ\text{-}700^\circ\text{C}$  for 2-4 h. The PZT crystallites were in near spherical shapes. Their average size varied in the 16-25 nm range according to the final temperature. Such small crystallites obtained in this particular method had a rather simple X-ray diffraction in a new tetragonal crystal structure in comparison to the well-known rhombohedral structure in the Zr-rich PZTs or that of the tetragonal structure in the Ti-rich PZTs. Both of them had a much complicated X-ray diffraction with vacancies in B as well as the A sublattice sites. Abreu *et al.* (2004) synthesized PZT/ $\text{Pb}(\text{Zr}_{0.52}\text{Ti}_{0.48})\text{O}_3$  by a chemical method using the conventional Pechini method and the urea-modified Pechini method, based on the formation of metallic complexes with carboxylic acid, normally citric acid, followed by a polymerization reaction with a polyalcohol, normally ethylene glycol, generating polyester and obtained sub-micrometric spherical particles of  $0.1\ \mu\text{m}$  and a  $7.4\ \text{m}^2/\text{g}$  surface area. Wang *et al.* (2004) characterized hydrothermally and synthesized lead zirconate titanate or PZT ceramic at  $220^\circ\text{C}$  for 24 h with a mineralizer KOH concentration of 1.6 M.

Chao *et al.* (2001) synthesized lead zirconate titanate nanoparticle from lead acetate, Titanium (IV) ethoxide, and zirconium (IV) butoxide by sol-gel. The PZT or  $\text{Pb}(\text{Zr}_{0.5}\text{Ti}_{0.5})\text{O}_3$  nanoparticles currently obtained varied in sizes from about 10 to 30 nm. Zhang *et al.* (2002) prepared  $\text{Pb}(\text{Zr}_{0.52}\text{Ti}_{0.48})\text{O}_3$  by a hybrid method of the sol-gel and solid-state reaction. Reaction of the oxides to PZT occurred at a temperature as low as  $500^\circ\text{C}$ , which is believed to be induced by the PZT crystallized from the sol-gel portion in the system. Fully dense PZT ceramics with 99% of the theoretic density have been achieved from the partially reacted mixture at a sintering temperature of  $1100^\circ\text{C}$  for 1h. The good dielectric ( $K=1030, \delta=3\%$ ) and ferroelectric ( $P_r = 24.3\ \mu\text{C}/\text{cm}^2, E_c = 12\text{kV}/\text{cm}$ ) properties of the sintered PZT ceramics. Chen *et al.* (2003) studied the effect of seeds on the lead zirconate titanate (PZT/ $\text{Pb}(\text{Zr}_{0.52}\text{Ti}_{0.48})\text{O}_3$ ) powders fabricated by a sol-gel processing with a thermal analysis, and followed by transmission electron microscopy analysis. Zirconium (IV) propoxide, titanium (IV) isopropoxide and lead (II) acetate trihydrate were used as starting materials. A low temperature phase transformation of  $450^\circ\text{C}$  from pyrochlore

(Py) to perovskite (Pe) was observed. It can be concluded that the introduction of seeds into system does not suppress the formation of the metastable pyrochlore phase. However, the seeds reduce the energy barrier for pyrochlore phase transformation to the desired perovskite phase and thus facilitate the creation of perovskite phase. As a result, the pyrochlore phase can be eliminated quickly at low temperature. Xu *et al.* (2004) synthesized lead zirconate titanate (PZT)(52/48) powders by a hybrid method of sol-gel and ultrasonic atomization. The starting materials used were lead acetate trihydrate (99.5% purity), zirconium dioxide (99.22% purity), titanium (IV) isopropoxide (98% purity) and citric acid. The PZT ceramics sintered at 1150°C for 4 h exhibited a relative density of 98.5%, a piezoelectric coefficient of 221 pC/N, a remnant polarization of 24.1  $\mu\text{C}/\text{cm}^2$ , and a coercive field of 10.1 kV/cm. The Curie temperature ( $T_c$ ), room temperature and maximum dielectric constants of PZT sample are 390°C, 900 and 8600, respectively at 1 kHz.